Journal of Thermal Analysis and Calorimetry (2020) 142:1223–1231
https://doi.org/10.1007/s10973-020-09632-9

Use of slag (GBFS) generated in charcoal blast furnace as raw material in alkali-activated cement

E. A. Langaro[1] · M. Costa de Moraes[2] · I. S. Buth[2] · C. Angulski da Luz[2] · J. I. Pereira Filho[2] · A. Matoski[1]

Received: 26 July 2019 / Accepted: 24 March 2020 / Published online: 5 April 2020

Abstract
Alkali-activated cements are low-environmental-impact binders and can be obtained from the alkaline activation of wastes such as slags and fly ashes, and solutions of hydroxides and silicates. In this study, two types of slag, A and B, generated in charcoal and coke blast furnaces, respectively, were activated with NaOH in contents of 4, 5 and 6% to obtain alkali-activated slag (AAS). Samples were submitted to calorimetry and compressive strength tests, and investigative microstructure analysis. The results showed that cement obtained with slag A (AAS_A) presented a much superior performance than AAS_B, which was related to the higher degree of hydration, higher formation of amorphous CSH with a higher incorporation of aluminum ions (C–(A)S–H). For AAS_B, the activator content was not able to improve the compressive strength. Calorimetry measurements showed a small interaction between slag B and the activator. The results contribute to the appreciation of slags generated in charcoal blast furnaces, which may become raw material for low-environmental-impact cements, in this case, AAS.

Keywords Alkali-activated slag · Granulated blast-furnace slag · Microstructure · Calcium silicate hydrate (C–S–H)

Introduction

The concrete industry contributes around 7% to total global CO_2 emissions and approximately 90% of this embodied energy and associated carbon is due to the commonly used Portland cement binder [1]. Relative to other building materials, concrete has a low embodied energy and carbon footprint. However, due to the enormous quantity of concrete used each year, the resulting total embodied energy and carbon footprint is quite large.

Alkali-activated cements can only be synthesized from waste without the need for the calcination process. Alkali-activated cements are usually obtained from slag, fly ash or metakaolin, which are activated by solutions of sodium hydroxide (NaOH), potassium hydroxide (KOH) and silicates. Raw materials rich in SiO_2 and Al_2O_3 form an amorphous aluminosilicate material as a hydrated compound, while those rich in CaO produce calcium silicate hydrate (C–S–H) [2–5].

In the alkali-activated slag (AAS) obtained from the granulated blast-furnace slag (GBFS), the main hydration product is C–S–H, or C–A–S–H, due to the incorporation of Al_2O_3 in its structure [6–8]. Hydrotalcite, merwinite, stratlingite and calcium monosulfoaluminate hydrate may also be present as minority phases [9–15].

One of the most important characteristics of slags in order to obtain binders is the ratio between CaO and SiO_2 contents, also known as the simplified basicity index, which classifies them as acidic or basic if the value is lower or higher than one, respectively ($CaO/SiO_2 < 1$: acidic; $CaO/SiO_2 > 1$: basic). The importance of CaO is due to the origin of coal used in blast furnaces. The slags from coal blast furnaces (coke) are considered basic, taking into account the need for a large percentage of CaO to remove the present sulfur. On the other hand, those produced in charcoal blast furnaces, where the sulfur content is low, have a low CaO/SiO_2 ratio and are usually considered acidic [16]. In Brazil, 20% of annual steel production is from charcoal [17], with growth prospects due to the increase in the use of charcoal as a substitute for coke. The Brazilian standard concerning the use of slags as supplementary material in Portland cements [18]

✉ C. Angulski da Luz
angulski@utfpr.edu.br

[1] Departamento de Engenharia Civil, Universidade Tecnológica Federal do Paraná, Campus Curitiba, Curitiba, PR, Brazil

[2] Departamento de Engenharia Civil, Universidade Tecnológica Federal do Paraná, Campus Pato Branco, Pato Branco, PR 85501970, Brazil

considers the ratio $CaO + MgO + Al_2O_3/SiO_2$ as the basicity index. Due to their chemical characteristics, only the basic slags end up being used as raw material in the production of blast-furnace Portland cements, while the acidic slags are deposited in steel company yards. The performance of different blast-furnace slags in Portland cements, supersulfated cements and AAS has been the object of study in recent papers [13–15, 19, 20]. In relation to AAS, Ben Haha et al. [14] observed that when it was activated by water glass, the MgO content in slag contributed to the reduction in porosity and the increase in compressive strength and hydrotalcite formation, as well as a lower incorporation of Al ions in C–SH. However, when NaOH was used as an activator, only a slight increase in the compressive strength was noticed. On the contrary, a higher content of Al_2O_3 in slag implied a higher incorporation of Al in C–S–H, delayed the initial hydration and reduced the compressive strength [15]. In a recent paper, Cadore et al. [21] investigated the carbonation of AAS made from GBFS generated by charcoal. They verified that AAS presented a high carbonation and a drop in compressive strength, which was related to the decalcification of CSH and the formation of vaterite. They observed that although the slag from charcoal had more Al_2O_3 and MgO, it was unable to form aluminosilicate or hydrotalcite, which could reduce the susceptibility of AAS carbonation. Langaro et al. [22] also investigated the behavior of AAS made from charcoal-generated GBFS and compared it with a slag from coke. They used 5% alkaline activator and observed a better compressive strength for AAS made from charcoal. However, the formation of hydrotalcite was only evidenced in AAS made from coke.

This study aims to contribute to the understanding of the type of slag in AAS and, above all, to contribute to the appreciation of slags generated in charcoal blast furnaces. Therefore, two slags (from charcoal and from coke) were activated with NaOH in contents of 4, 5 and 6% to obtain alkali-activated slag (AAS). The effect of the chemical composition of slag and activator content on the microstructures and mechanical properties was investigated.

Materials and methods

Two granulated blast-furnace slags with different chemical compositions were used to produce AAS, one from a charcoal blast furnace (acidic [A]) and another from a coke blast furnace (basic [B]). Both slags were oven-dried for approximately 24 h at a controlled temperature of 105 °C. Then, they were ground in a ball mill for 2 h. The chemical composition determined by X-ray fluorescence (Table 1) shows that the slag generated in a charcoal blast furnace (acidic) has a lower CaO/SiO_2 ratio than the basic one, as expected.

Table 1 Chemical composition and physical properties of slag A and B

Oxides/%	Slag A	Slag B
SiO_2	38.1	32.2
CaO	37.0	49.5
Al_2O_3	13.9	8.2
MgO	6.2	5.0
Fe_2O_3	1.3	0.8
MnO	1.1	1.3
K_2O	0.9	0.5
TiO_2	0.8	0.6
Na_2O	0.2	0.1
SO_3	0.1	1.4
CaO/SiO_2	0.97	1.54
$CaO + MgO + Al_2O_3/SiO_2$*	1.50	1.95
Physical properties		
Bulk density/g/cm^3	2.55	2.92
Blaine specific surface area/cm^2/g	5352	4410

*NBR 5735

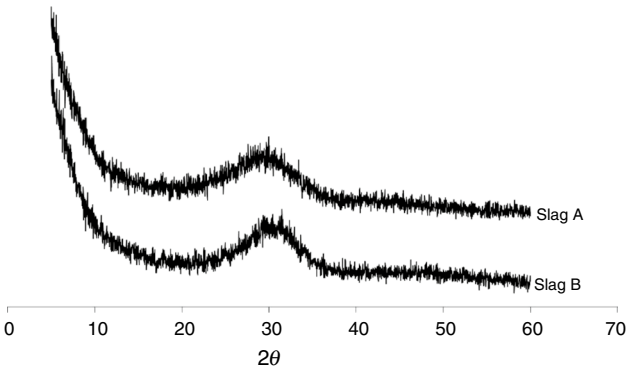

Fig. 1 X-ray diffractograms of slags A and B

However, both meet the Brazilian standard for their use as supplementary material cement in Portland Cement according to NBR 16697 [18]. Slag A also presents higher MgO and Al_2O_3 contents, mainly the latter. Figure 1 confirms the amorphous characteristics of both slags. It is also observed that, even if ground for the same amount of time, slag A presented a larger specific surface area (Table 1) and a finer grain size distribution (Fig. 2).

For the production of AAS, NaOH was used as the activator at 4, 5 and 6% in relation to the slag mass. For the pastes, the water-to-slag ratio (w s^{-1}) was 0.4 and for mortars, the proportion was 1:2.75:0.485 (slag: aggregate: water, in mass), according to ASTM [23]. In both pastes and mortars, the activator was mixed with water beforehand to ensure a good distribution in the mixture.

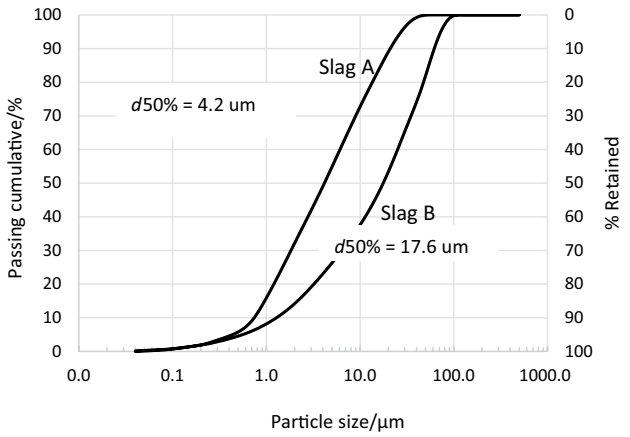

Fig. 2 Grain size distribution of slags A and B

The mortars were molded in triplicate prismatic specimens, maintained in an environment with a minimum relative humidity of 95% at 23 °C and analyzed at 7, 28 and 90 days.

The study of the microstructure was performed in pastes with a w–s ratio of 0.4. For the isothermal conduction calorimetry test, the Calmetrix calorimeter, model I-Cal 2000 HPC, was used for 7 days at 23 °C. From the curves, the periods of induction and setting times were determined according to Betioli et al. [24].

For the X-ray diffraction (XRD), differential scanning calorimetry (DSC) and scanning electron microscopy (SEM) tests, the hydration was interrupted at 7, 28 and 90 days. The samples were initially fragmented and immersed in acetone for 2 h, which was extracted with the aid of a vacuum pump; then, the samples were kept at a controlled temperature of 40 °C for 24 h, according to Angulski da Luz and Hooton [20]. For the XRD and DSC analyses, the samples were ground into particles of less than 150 um.

The XRD samples were performed under the following conditions: Cu-Kα radiation tube, wavelength of 1.54 Ă (40 kV, 25 mA), in the range of 5°–70° (2θ), with a step size of 0.02°, time of 10 s.

The thermal differential scanning calorimetry (DSC) analyses were performed under the following conditions: 30–600 °C range, with a heating rate of 10 °C min^{-1}, a synthetic air

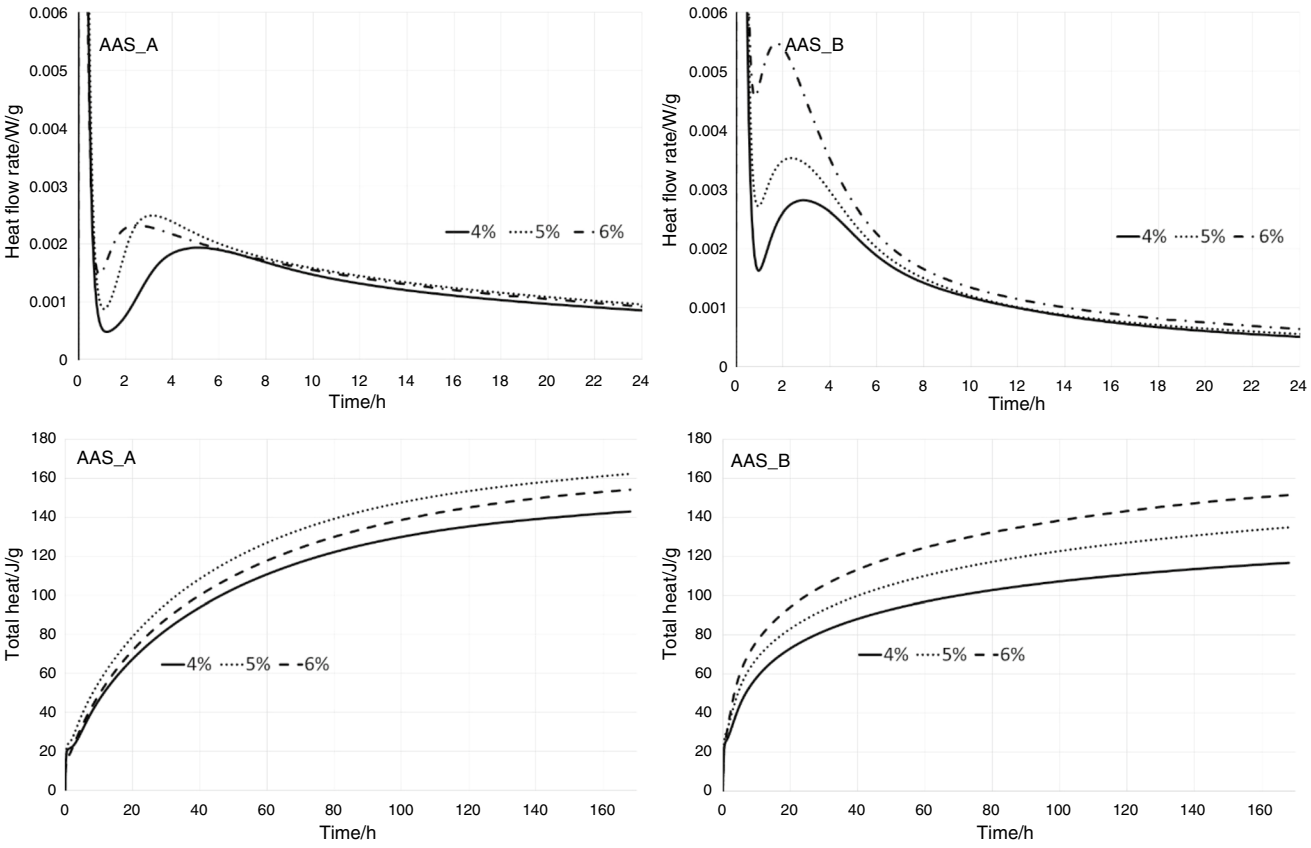

Fig. 3 Isothermal calorimetric measurements: heat flow rate and total heat for AAS_A and AAS_B containing 4, 5 and 6% of NaOH up to 7 days

Table 2 Duration of induction period, setting times and maximum flow for AAS_A and AA_B containing 4, 5 and 6% of alkaline activator (NaOH) obtained from Fig. 3

AAS	NaOH/%	Induction period		Main peak	
		Total period/h:min	Initial setting time/h:min	Maximum flow/KW/g × 10^{-6}	Final setting time/h:min
AAS_A	4	00:55	01:33	1.93	05:07
	5	00:37	01:15	2.49	03:08
	6	00:22	00:59	2.32	02:53
AAS_B	4	00:27	01:03	2.81	02:54
	5	00:24	01:03	3.53	02:21
	6	00:19	00:54	5.47	01:42

atmosphere and a flow of 100 mL min^{-1}. To determine the mass loss, the samples were weighed before and at the end of the analysis.

For the observation of the samples in the SEM, the preparation of the samples consisted of the application of vacuum and metallization with gold.

Results

Heat of hydration

The heat of hydration of AAS made with slags A and B (AAS_A and AAS_B) containing 4, 5 and 6% NaOH was monitored for a period of 168 h (Fig. 3).

The first peak corresponds to the initial dissolution of the slag and activator. The induction period between the two peaks is characterized by a low rate of released heat, which is the consequence of a period of low reactivity. The second peak corresponds to the main peak or peak of hydration, which is of high reactivity. This is where the precipitation of the hydrated products takes place, in this case the C–S–H. It is possible to observe that both cements had intense dissolution peaks and short periods of induction (Table 2).

In relation to the type of slag, the AAS_A cements presented less intense peaks of hydration. However, they were more extensive, showing a more gradual heat release and, consequently, a higher accumulated heat and a higher reactivity at the end of 7 days.

For AAS_A, the activator content had a greater influence on the position (time) of the main peak: The higher the activator content before the main peak occurred, the more the final setting time (which corresponds to the peak point) was reduced. For AAS_B, the effect of the activator content was on the intensity of the main peak, which increased as the activator content increased. In general, it could be noted that the influence of the activator content on the hydration kinetics was more intense for slag A, while for slag B, the released heat seemed more related to heat from the activator itself, showing little interaction with slag B.

Compressive strength

The AAS produced with slag A (AAS_A) obtained much higher compressive strength results than AAS_B, mainly at 28 and 90 days, while for slag B (AAS_B), the values were lower than 15 MPa, even at 90 days (Fig. 4). The effect of slag type can be compared with those observed by Ben Haha [14], who noticed that the content of MgO increased the compressive strength. The authors attributed this increase to a higher formation of hydrotalcite and lower porosity in AAS with high MgO content. However, in relation to Al_2O_3 content, Ben Haha [15] observed a slight decrease in

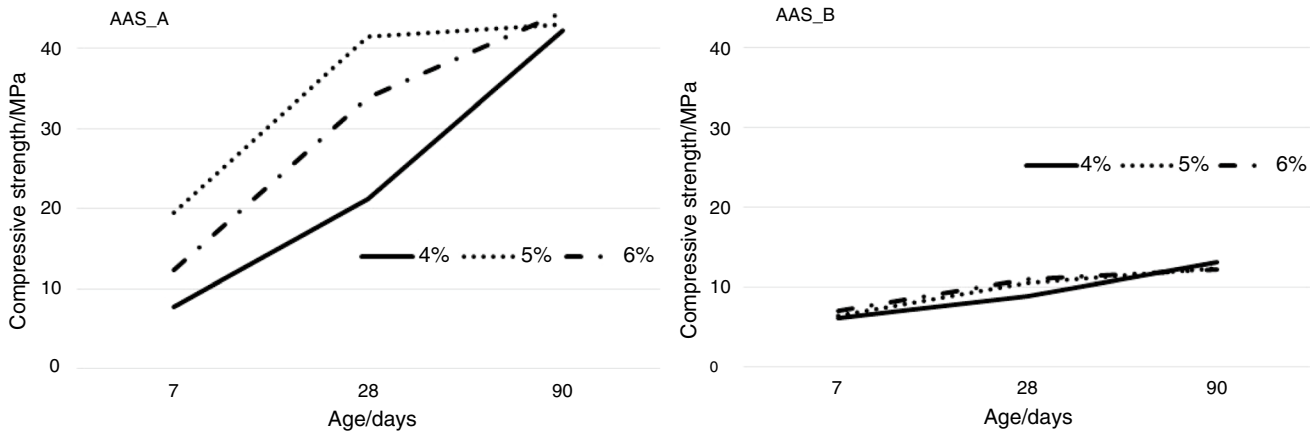

Fig. 4 Compressive strength for AAS_A and AAS_B containing 4, 5 and 6% of NaOH at 7, 28 and 90 days

compressive strength as Al_2O_3 increased. In this study, slag A had higher content of both MgO (A: 5.0% and B: 6.2%) and Al_2O_3 (A:13.9 and B: 8.2%), mainly the latter, showing disagreement with the literature regarding the alumina content [15].

For slag A, the activator content (NaOH) was significant at 7 and 28 days and had a similar effect as observed on accumulated heat at 7 days (4%: 7.7 MPa and 140 J g^{-1}; 5%: 19.4 MPa and 160 J g^{-1}; 6%: 12.3 MPa and 155 J g^{-1}). This showed that 5% NaOH was the best dosage (higher values), while 4% was too little and 6% was too much. However, at 90 days, the values of all dosages reached compressive strength close to 40 MPa. For AAS_B, the activator content was not able to improve the compressive strength at any age. This behavior was also consistent with

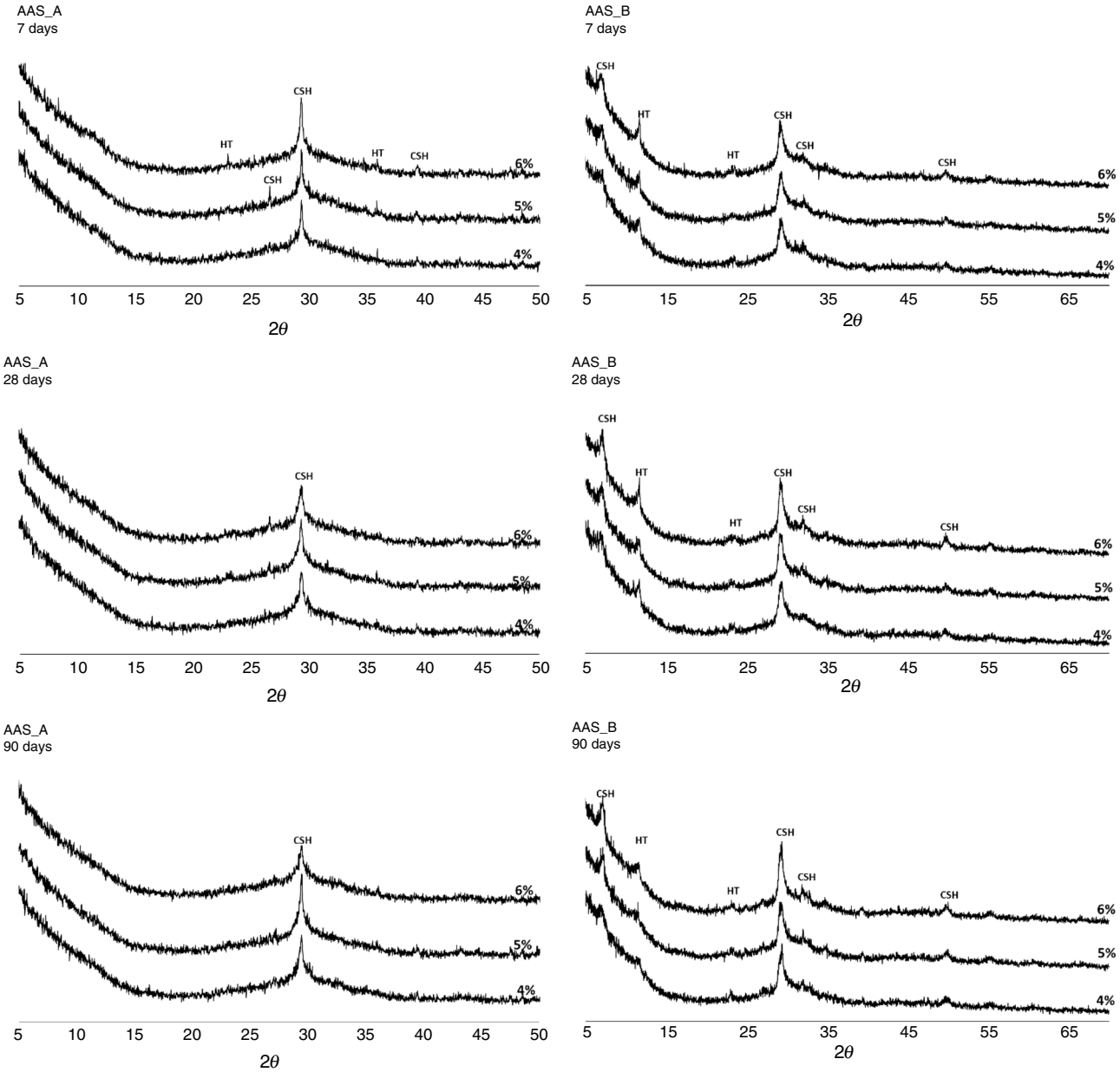

Fig. 5 XRD analyses for AAS_A and AAS_B containing 4, 5 and 6% of NaOH at 7, 28 e 90 days, *CSH* calcium silicate hydrated e *HT* hydrotalcite

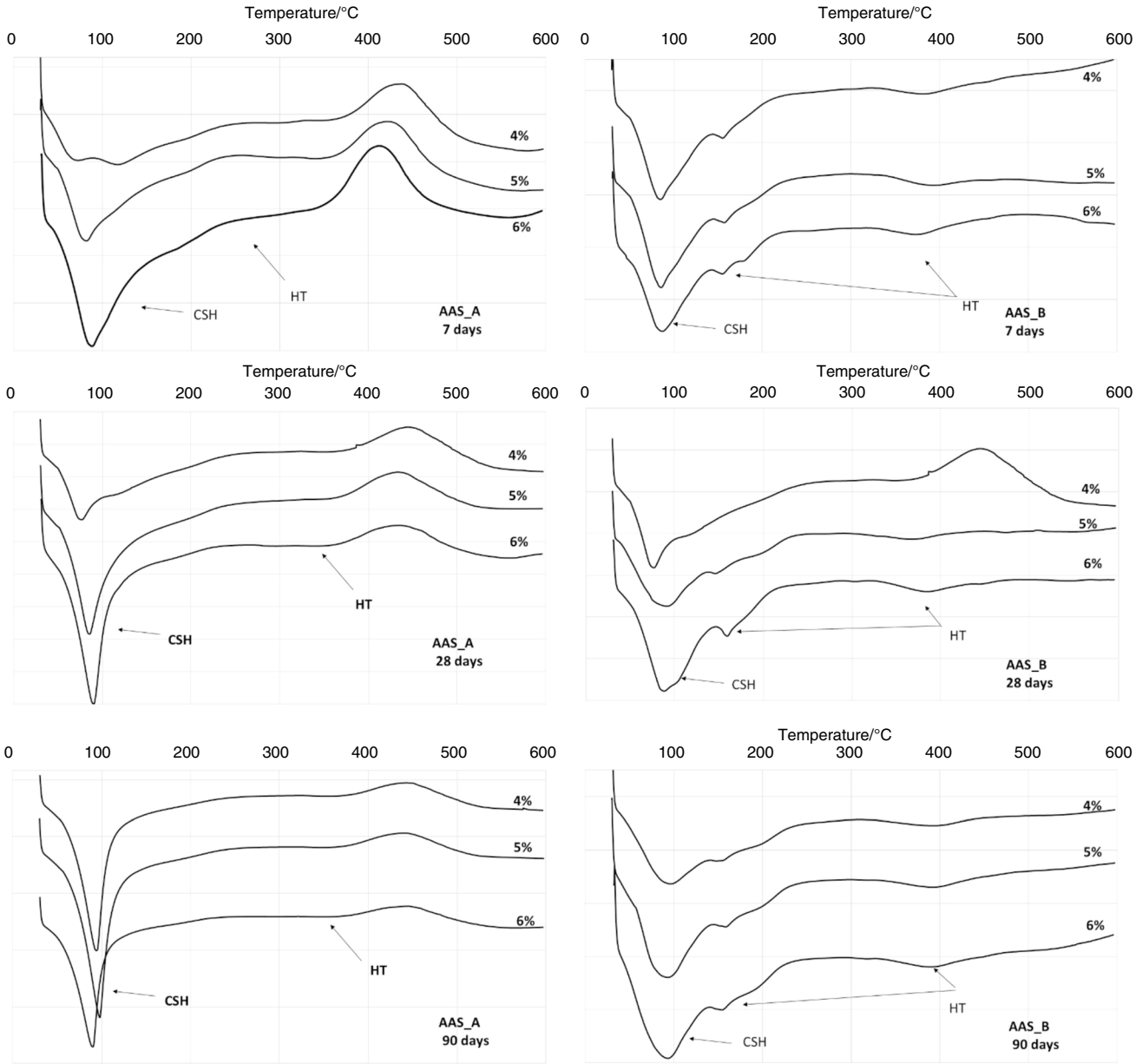

Fig. 6 DSC analyses for AAS_A and AAS_B containing 4, 5 and 6% of NaOH at 7, 28 e 90 days, *CSH* calcium silicate hydrated e *HT* hydrotalcite

Table 3 Total mass loss obtained from DSC analyses for AAS_A and AA_B containing 4, 5 and 6% of alkaline activator (NaOH)

Age/days	AAS_A			AAS_B		
	NaOH			NaOH		
	4%	5%	6%	4%	5%	6%
7	8.85	11.49	13.02	10.10	11.05	12.34
28	11.96	15.23	15.15	11.98	12.69	13.18
90	17.01	19.14	16.62	10.41	12.71	13.46

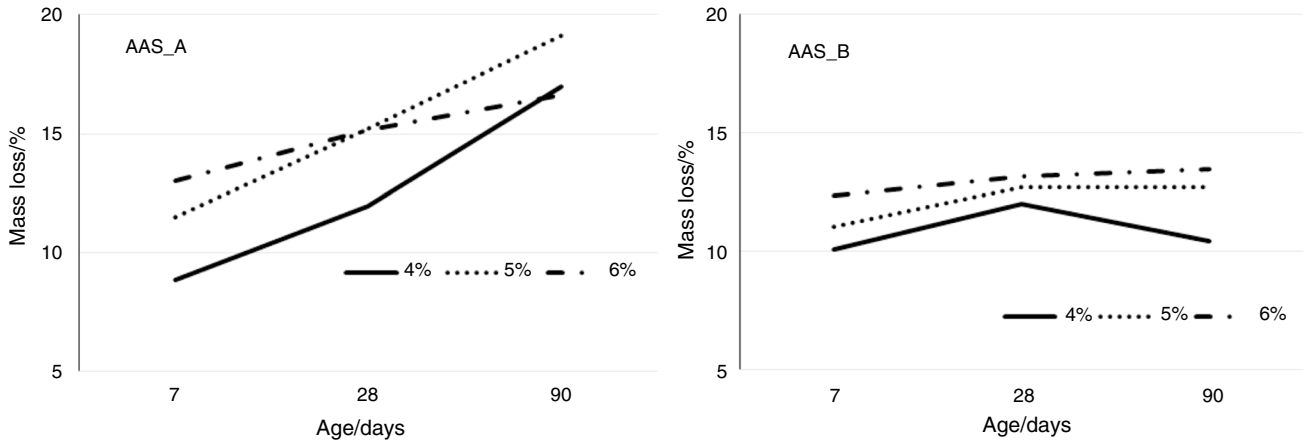

Fig. 7 Mass loss for AAS_A and AAS_B containing 4, 5 and 6% of NaOH at 7, 28 and 90 days

calorimetry measurements that showed little interaction between slag B and the activator.

Microstructure

Figure 5 shows the diffractograms of the pastes made with AAS with slags A and B, respectively, at 7, 28 and 90 days. It is possible to observe the presence of C–S–H in all pastes and at all ages. AAS-B presents more peaks, including CSH, evidencing a less amorphous system. In this sense, the higher content of Al_2O_3 present in slag A could contribute to the incorporation of Al in C–S–H, making the system more amorphous as observed by Ben HaHa et al. [15]. The presence of hydrotalcite also predominates only in those with slag B and was related to the presence of MgO in slag [14, 15].

The DSC analyses of the AAS-A and AAS-B pastes at 7, 28 and 90 days, exhibited in Fig. 6, confirmed the presence of CSH (peak close to 100 °C) in all samples. However, hydrotalcite (peak close to 150 °C and 400 °C) was only observed in the AAS_B pastes, as also noticed in XRDs [13–15]. The total mass loss determined in the DSC analyses is presented in Table 3, showing that the degree of hydration of the AAS_A samples at 28 and (mainly) 90 days is higher than that of the AAS_B samples. It also shows that in the AAS_A samples, the highest degree of hydration occurs with 5% of the activator. The degree of hydration presented a similar behavior to those observed in compressive strength in relation to the type of slag and also the activator content (Fig. 7).

SEM images show that C–S–H was found in all samples of both slags (Fig. 8). In the AAS_A pastes, the C–S–H was observed as a gel with a small crystalline structure. In the AAS_B pastes, a more reticulated structure was observed and found more easily.

The morphology of C–S–H observed in AAS may be compared to types I and II [25]. Type I is more evident in pastes with slag A. On the other hand, type II is very similar to the slag B pastes. The EDS analyses in Table 4, show that C(A)–S–H formed in the AAS_A pastes presents a higher incorporation of aluminum ions (higher Al/Si ratio) than the one formed in the pastes made with AAS_B, regardless of the activator content. The Ca/Si ratio is slightly higher in the C(A)–S–H formed in AAS_A, and the presence of Mg ions is also higher. The analyses indicate that the higher Al_2O_3 content in slag A combined with its higher reactivity may have promoted the incorporation of Al in C–S–H, thus avoiding the formation of hydrotalcite. On the contrary, in

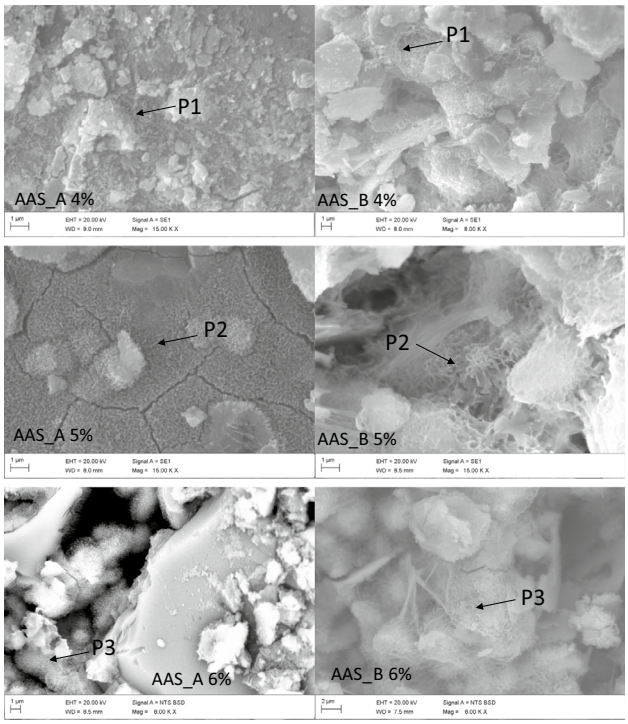

Fig. 8 SEM images for AAS_A and AAS_B containing 4, 5 and 6% of NaOH at 7 days

pastes made with AAS_B, which is clearly less reactive, the low CSH formation allowed the Al and Mg ions to form the hydrotalcite ($Mg_6Al_2(OH)16CO_3{\cdot}4H_2O$), since little CSH was formed (low degree of hydration).

Conclusions

In this paper, two blast-furnace slags, A (from charcoal) and B (from coke), were studied as raw material to obtain alkali-activated slag (AAS). Three NaOH contents were investigated. From the obtained results, it is possible to draw the following conclusions:

- The chemical composition of GBFS was the main factor responsible for the performance of the alkali-activated cement, regardless of the amount of the activator. AAS made from GBFS generated in charcoal blast furnaces (AAS_A) presented the compressive strength results much higher than those presented by slag B (from coal). For AAS_B, the activator content was not able to improve the compressive strength;
- The better performance of AAS_A was due to the higher formation of hydrated compounds (higher degree of hydration), the type of hydrated compounds

Table 4 EDS analyses of SEM images for AAS_A and AA_B containing 4, 5 and 6% of alkaline activator (NaOH)

NaOH	AAS_A			AAS_B		
	4%	5%	6%	4%	5%	6%
Point	P1	P2	P3	P1	P2	P3
Composition/%						
Na	1.71	2.93	4.2	7.23	4.35	7.29
Mg	3.13	3.66	2.75	1.83	1.79	1.6
Al	6.8	6.9	4.74	2.18	2.4	2.53
Si	16.36	16.47	10.85	8.61	9.54	8.97
Ca	17.39	19.95	7.48	11.42	13.89	12.55
Mn	0.43	0.64	0.27	0.28	0.33	0
Ratios						
Ca/Si	1.06	1.21	0.69	1.33	1.46	1.40
Al/Si	0.42	0.42	0.44	0.25	0.25	0.28

and the type of CSH formed. In the AAS_A pastes, the presence of amorphous CSH was mostly identified. The higher content of Al_2O_3 in slag A, in addition to its higher reactivity, would have promoted the incorporation of Al ions in C(A)–S–H, thus avoiding the formation of hydrotalcite. On the contrary, in the pastes made with AAS_B, the low CSH formation enabled the Al and Mg ions to form hydrotalcite;

- The performance of AAS is strongly dependent on the type of raw material. The basicity indexes that prioritize the presence of CaO do not serve as a basis for classifying slag as suitable or not suitable for use in AAS. The Al_2O_3 content has been fundamental for the analysis of slag as a raw material;
- The study of the influence of the chemical composition of slag on cements contributes to the appreciation of those generated from charcoal blast-furnace slags, which may not be attractive to Portland cement. However, they may become raw material for low-environmental-impact cements, in this case, alkali-activated slag (AAS).

Acknowledgements The authors wish to thank the CNPq (National Counsel of Technological and Scientific Development Grant No. 483661/2013-9) and the CAPES (Coordination for the Improvement of Higher Education Personnel) in Brazil for their support.

References

1. Limbachiya M, Can Bostanci S, Kew H. Suitability of BS EN 197-1 CEM II and CEM V cement for production of low carbon concrete. Constr Build Mater. 2014;71:397–405.
2. Xu H, van Deventer JSJ. Geopolymerisation of multiple minerals. Miner Eng. 2002;15:1131–9.
3. Pacheco-Torgal F, Castro-Gomes J, Jalali S. Alkali-activated binders: a review. Part 2. About materials and binders manufacture. Constr Build Mater. 2008;22:1315–22.
4. Shi C, Fernández-Jiménez A, Palomo A. New cements for the 21st century: the pursuit of an alternative to Portland cement. Cem Concr Res. 2011;41:750–63.
5. Reig L, Soriano L, Borrachero MV, Monzó J, Payá J. Influence of the activator concentration and calcium hydroxide addition on the properties of alkali-activated porcelain stoneware. Constr Build Mater. 2014;63:214–22.
6. Li C, Sun H, Li L. A review: the comparison between alkali-activated slag (Si + Ca) and metakaolin (Si + Al) cements. Cem Concr Res. 2010;40:1341–9.
7. Schneider J, Cincotto MA, Panepucci H. 29Si and 27Al high resolution NMR characterization of calcium silicate hydrate phases in activated blast-furnace slag pastes. Cem Concr Res. 2001;31:993–1001.
8. Wang SD, Scrivener KL. Hydration products of alkali activated slag cement. Cem Concr Res. 1995;25:561–71.
9. Roy DM. Alkali-activated cements opportunities and challenges. Cem Concr Res. 1999;29:249–54.
10. Chen W, Brouwers HJH. The hydration of slag, part 1: reaction models for alkali-activated slag. J Mater Sci. 2007;42:428–43.
11. Gruskovnjak A, Lothenbach B, Holzer L, Figi R, Winnefeld F. Hydration of alkali-activated slag: comparison with ordinary Portland cement. Adv Cem Res. 2006;18:119–28.
12. Gong K, White CE. Impact of chemical variability of ground granulated blast-furnace slag on the phase formation in alkali-activated slag pastes. Cem Concr Res. 2016;89:310–9.
13. Ben Haha M, Le Saout G, Winnefeld F, Lothenbach B. Influence of activator type on hydration kinetics, hydrate assemblage and microstructural development of alkali activated blast-furnace slags. Cem Concr Res. 2011;41:301–10.
14. Ben Haha M, Lothenbach B, Le Saout G, Winnefeld F. Influence of slag chemistry on the hydration of alkali-activated blast-furnace slag—part I: effect of MgO. Cem Concr Res. 2011;41:955–63.
15. Ben Haha M, Lothenbach B, Le Saout G, Winnefeld F. Influence of slag chemistry on the hydration of alkali-activated blast-furnace slag—part II: effect of Al2O3. Cem Concr Res. 2012;42:74–83.
16. Langaro E, Buth IS, Moraes MC, Angulski Da Luz C, Matoski A, Pereira Filho JI, Effect of NaOH content in activated alkali cement (AAC) made with basic slag. In: Materiales sostenibles para un mundo viviente sustainable materials for a living world, 2016, Cali, Colômbia. 6th Amazon & Pacific green materials congress and sustainable construction materials lat—Rilem Conference (2016), pp. 614–622.
17. Sindifer, Syndicate of iron industry in the state of minas Gerais. Annual Report (2015).
18. Associação Brasileira De Normas Técnicas. NBR 16697. Cimento Portland—Requisitos. Rio de Janeiro, p 12 (2018).
19. Ogirigbo OR, Black L. Influence of slag composition and temperature on the hydration and microstructure of slag blended cements. Constr Build Mater. 2016;126:496–507.
20. Angulskida Luz C, Hooton RD. Influence of curing temperature on the process of hydration of supersulfated cements at early age. Cem Concr Res. 2015;77:69–75.
21. Cadore DE, Da Luz CA, De Medeiros MHF. An investigation of the carbonation of alkaline activated cement made from blast furnace slag generated by charcoal. Constr Build Mater. 2019;226:117–25.
22. Langaro EA, Da Luz CA, Buth IS, De Moraes MC, Pereira Filho JI, Matoski A. The influence of chemical composition and fineness on the performance of alkali activated cements obtained from blast furnace slags. Matéria. 2017;22:1–11.
23. American Society for Testing and Materials—ASTM, Standard specification for compressive strength of hydraulic cement mortars (Using 2-in. or [50-mm] cube specimens), ASTM C109/C, West Conshohocken, PA, United States (2008).
24. Betioli AM, Gleize PJP, John VM, Pileggi RG. Effect of EVA on the fresh properties of cement paste. Cement Concr Compos. 2012;34:255–60.
25. Taylor HFW. Cement chemistry. 2nd ed. New York: Thomas Telford; 1997.